

1 **SYNERGY BETWEEN SATELLITE OBSERVATIONS OF SOIL MOISTURE**
2 **AND WATER STORAGE ANOMALIES FOR RUNOFF ESTIMATION**

3 Stefania Camici ⁽¹⁾, Gabriele Giuliani ⁽¹⁾, Luca Brocca ⁽¹⁾, Christian Massari ⁽¹⁾, Angelica Tarpanelli
4 ⁽¹⁾, Hassan Hashemi Farahani ⁽²⁾, Nico Sneeuw ⁽²⁾, Marco Restano ⁽³⁾, Jérôme Benveniste ⁽⁴⁾

5 *(1) National Research Council, Research Institute for Geo-Hydrological Protection, Perugia, Italy (s.camici@irpi.cnr.it)*

6 *(2) Institute of Geodesy, University of Stuttgart, Geschwister-Scholl-Straße 24D, 70174 Stuttgart, Germany*

7 *(3) SERCO c/o ESA-ESRIN, Largo Galileo Galilei, Frascati, 00044, Italy*

8 *(4) European Space Agency, ESA-ESRIN, Largo Galileo Galilei, Frascati, 00044, Italy*

9

10

11

12

13

14

15

16

17

18

November 2020

19

Submitted to:

20

* Correspondence to: Ph.D. Stefania Camici, Research Institute for Geo-Hydrological Protection, National Research Council, Via della Madonna Alta 126, 06128 Perugia, Italy. Tel: +39 0755014419 Fax: +39 0755014420 E-mail: stefania.camici@irpi.cnr.it.

21 **ABSTRACT**

22 This paper presents an innovative approach, STREAM - SaTellite based Runoff Evaluation And
23 Mapping - to derive daily river discharge and runoff estimates from satellite soil moisture,
24 precipitation and terrestrial water storage anomalies observations. Within a very simple model
25 structure, the first two variables (precipitation and soil moisture) are used to estimate the quick-flow
26 river discharge component while the terrestrial water storage anomalies are used for obtaining its
27 complementary part, i.e., the slow-flow river discharge component. The two are then summed up to
28 obtain river discharge and runoff estimates.

29 The method is tested over the Mississippi river basin for the period 2003-2016 by using Tropical
30 Rainfall Measuring Mission (TRMM) Multi-satellite Precipitation Analysis (TMPA) precipitation
31 data, European Space Agency Climate Change Initiative (ESA CCI) soil moisture data and Gravity
32 Recovery and Climate Experiment (GRACE) terrestrial water storage data. Despite the model
33 simplicity, relatively high-performance scores are obtained in river discharge simulations, with a
34 Kling-Gupta efficiency index greater than 0.65 both at the outlet and over several inner stations used
35 for model calibration highlighting the high information content of satellite observations on surface
36 processes. Potentially useful for multiple operational and scientific applications (from flood warning
37 systems to the understanding of water cycle), the added-value of the STREAM approach is twofold:
38 1) a simple modelling framework, potentially suitable for global runoff monitoring, at daily time scale
39 when forced with satellite observations only, 2) increased knowledge on the natural processes, human
40 activities and on their interactions on the land.

41

42 Key words: satellite products, soil moisture, water storage variations, conceptual hydrological
43 modelling, rainfall-runoff modelling, Mississippi.

44 1. INTRODUCTION

45 Spatial and temporal continuous river discharge monitoring is paramount for improving the
46 understanding of the hydrological cycle, for planning human activities related to water use as well as
47 to prevent/mitigate the losses due to extreme flood events. To accomplish these tasks, runoff and river
48 discharge data, which represents the aggregated signal of runoff (Fekete et al., 2012), should be
49 available at adequate spatial/temporal resolution, i.e., at basin scale (basin area larger than 10'000
50 km²) and at monthly time step for water resources management and drought monitoring up to grid
51 scale (few km)/(sub-) daily time step for flood prediction. The accurate continuous (in space and
52 time) runoff and river discharge estimation at finer spatial/temporal resolution is still a big challenge
53 for hydrologists.

54 Traditional in situ observations of river discharge, even if generally characterized by high temporal
55 resolution (up to sub-hourly time step), typically offer little information on the spatial distribution of
56 runoff within a watershed. Moreover, river discharge observation networks suffer from many
57 limitations such as low station density and often incomplete temporal coverage, substantial delay in
58 data access and large decline in monitoring capacity (Vörösmarty et al. 2002). Paradoxically, this
59 latter issue is exacerbated in developing nations (Crochemore et al, 2020), where the knowledge of
60 the terrestrial water dynamics deserves greater attention due to huge damages to settlements and
61 especially the loss of human lives that occurs regularly.

62 This precarious situation has led to growing interest in finding alternative solutions, i.e., model-based
63 or observation-based approaches, for runoff and river discharge monitoring. Model-based
64 approaches, based on the mathematical description of the main hydrological processes (e.g., water
65 balance models, WBMs, global hydrological models, GHMs, e.g., Döll et al., 2003 or, increasing in
66 complexity, land surface models, LSM, e.g., Balsamo et al., 2009; Schellekens et al., 2017), are able
67 to provide comprehensive information on a large number of relevant variables of the hydrological
68 cycle including runoff and river discharge at very high temporal and spatial resolution (up to hourly

69 sampling and 0.05° grid scale). However, the values of simulated water balance components rely on
 70 a massive parameterization of the soil, vegetation and land parameters, which is not always realistic,
 71 and are strongly dependent on the GHM/ LSM models used, analysis periods (Wisser et al., 2010)
 72 and climate forcings selected (e.g Haddeland et al., 2012; Gudmundsson et al., 2012a, b; Prudhomme
 73 et al., 2014; Müller Schmied et al., 2016).
 74 Alternatively, the observation-based approaches exploit machine learning techniques and a
 75 considerable amount of data to describe the physics of the system (i.e. hydraulic and/or hydrologic
 76 phenomena, Solomatine and Ostfeld, 2008) with only a limited number of assumptions. Besides being
 77 simpler than model-based approaches, these approaches still present some limitations. At first, as they
 78 rely on a considerable amount of data describing the modelled system's physics, the spatial/temporal
 79 extent and the uncertainty of the resulting dataset is determined by the spatial/temporal coverage and
 80 the accuracy of the forcing data (e.g., see E-RUN dataset, Gudmundsson and Seneviratne, 2016;
 81 GRUN dataset, Ghiggi et al., 2019; FLO1K dataset, Barbarossa et al., 2018). Additional limitations
 82 stem from the employed method to estimate runoff. Indeed, random forests such as employed in
 83 Gudmundsson and Seneviratne, 2016, like other machine learning techniques, are powerful tools for
 84 data driven modeling, but they are prone to overfitting, implying that noise in the data can obscure
 85 possible signals (Hastie et al., 2009). Moreover, the influence of land parameters on continental-scale
 86 runoff dynamics is not taken into account as the underlying hypothesis is that the hydrological
 87 response of a basin exclusively depend on present and past atmospheric forcing. It is easy to
 88 understand that this assumption will only be valid in certain circumstances and might lead to
 89 problems, e.g., over complex terrain (Orth and Seneviratne, 2015) or in cases of human river flow
 90 regulation (Ghiggi et al., 2019).
 91 Remote sensing can provide estimates of nearly all the climate variables of the global hydrological
 92 cycle including soil moisture (e.g., Wagner et al., 2007; Seneviratne et al., 2010), precipitation
 93 (Huffman et al., 2014) and total terrestrial water storage (e.g., Houborg et al., 2012; Landerer and
 94 Swenson, 2012; Famiglietti and Rodell, 2013). It has undeniably changed and improved dramatically

95 the ability to monitor the global water cycle and, hence, runoff. By taking advantage of satellite
96 information, some studies tried to develop methodologies able to optimally produce multivariable
97 datasets from the fusion of in situ and satellite-based observations (e.g., Rodell et al., 2015; Zhang et
98 al., 2018; Pellet et al., 2019). Other studies exploited satellite observations of hydrological variables,
99 e.g., precipitation (Hong et al., 2007), soil moisture (Massari et al., 2014), and geodetic variables (e.g.,
100 Sneeuw et al., 2014; Tourian et al., 2018) to monitor single components of the water cycle in an
101 independent way.

102 Although the majority of these studies provide runoff and river discharge data at basin scale and
103 monthly time step, they deserve to be recalled here as important for the purpose of the present study.
104 In particular, Hong et al. (2007) presented a first attempt to obtain an approximate but quasi-global
105 annual streamflow dataset, by incorporating satellite precipitation data in a relatively simple rainfall-
106 runoff simulation approach. Driven by the multiyear (1998-2006) Tropical Rainfall Measuring
107 Mission Multi-satellite Precipitation Analysis, runoff was independently computed for each global
108 land surface grid cell through the Natural Resources Conservation Service (NRCS) runoff curve
109 number (CN) method (NRCS, 1986) and subsequently routed to the watershed outlet to simulate
110 streamflow. The results, compared to the in situ observed discharge data, demonstrated the potential
111 of using satellite precipitation data for diagnosing river discharge values both at global scale and for
112 medium to large river basins. If, on the one hand, the work of Hong et al. (2007) can be considered
113 as a pioneer study, on the other hand it presents a serious drawback within the NRCS-CN method
114 that lacks a realistic definition of the soil moisture conditions of the catchment before flood events.
115 This aspect is not negligible, as it is well established that soil moisture is paramount in the partitioning
116 of precipitation into surface runoff and infiltration inside a catchment (Brocca et al., 2008). In
117 particular, for the same rainfall amount but different values of initial soil moisture conditions,
118 different flooding effects can occur (see e.g. Crow et al., 2005; Brocca et al., 2008; Berthet et al.,
119 2009; Merz and Blochl, 2009; Tramblay et al., 2010). On this line following Brocca et al. (2009),
120 Massari et al. (2016) presented a very first attempt to estimate global streamflow data by using

121 satellite Soil Moisture Active and Passive (SMAP, Entekhabi et al., 2010) and Global Precipitation
122 Measurement (GPM, [Huffman et al., 2019](#)) products. Although the validation was carried out by
123 routing the monthly surface runoff only in a single basin in Central Italy, the obtained results
124 suggested to dedicate additional efforts in this direction.

125 Among the studies that use satellite observations of hydrological variables for runoff estimation, the
126 hydro-geodetic approaches are undoubtedly worth mentioning, see e.g., ([Sneeuw et al., 2014](#)) for a
127 comprehensive overview or [Lorenz et al. \(2014\)](#) for an analysis of satellite-based water balance
128 misclosures with discharge as closure term. In particular, the satellite mission Gravity Recovery And
129 Climate Experiment (GRACE), which observed the temporal changes in the gravity field, has given
130 a strong impetus to satellite-driven hydrology research ([Tapley et al., 2019](#)). Since temporal gravity
131 field variations over the continents imply water storage change, GRACE was the first remote sensing
132 system to provide observational access to deeper groundwater storage. The relation between GRACE
133 groundwater storage change and runoff was characterized by [Riegger and Tourian \(2014\)](#), which even
134 allowed the quantification of absolute drainable water storage over the Amazon ([Tourian et al., 2018](#)).
135 In essence the storage-runoff relation describes the gravity-driven drainage of a basin and, hence, the
136 slow-flow processes. Due to GRACE's spatial-temporal resolution, runoff and river discharge are
137 generally available for large basins ($>160'000 \text{ km}^2$) and at monthly time step.

138 Based on the above discussion, it is clear that each approach presents strengths and limitations that
139 enable or hamper the runoff and river discharge monitoring at finer spatial and temporal resolutions.
140 In this context, this study presents an attempt to find an alternative method to derive daily river
141 discharge and runoff estimates at $\frac{1}{4}$ degree spatial resolution exploiting satellite observations and the
142 knowledge of the key mechanisms and processes that act in the formation of runoff, i.e., the role of
143 soil moisture in determining the response of a catchment to precipitation. For that, soil moisture,
144 precipitation and terrestrial water storage anomalies (TWSA) observations are used as input into a
145 simple modelling framework named STREAM v1.3 (SaTellite based Runoff Evaluation And
146 Mapping, version 1.3). Unlike classical land surface models, STREAM exploits the knowledge of the

147 system states (i.e., soil moisture and TWSA) to derive river discharge and runoff, and thus it 1) skips
148 the modelling of the evapotranspiration fluxes which are known to be a non-negligible source of
149 uncertainty (Long et al. 2014), 2) limits the uncertainty associated with the over-parameterization of
150 soil and land parameters and 3) implicitly takes into account processes, mainly human-driven (e.g.,
151 irrigation, change in the land use), that might have a large impact on the hydrological cycle and hence
152 on runoff.

153 The detailed description of the STREAM v1.3 model is given in section 4. The collected datasets and
154 the experimental design for the Mississippi River Basin (section 2) are described in sections 3 and 5,
155 respectively. Results, discussion and conclusions are drawn in section 6, 7 and 8, respectively.

156 **2. STUDY AREA**

157 The STREAM v1.3 model presented here has been tested and validated over the Mississippi River
158 basin. With a drainage area of about 3.3 million km², the Mississippi River basin is the fourth largest
159 watershed in the world, bordered to the West by the crest of the Rocky Mountains and to the East by
160 the crest of the Appalachian Mountains. According to the Köppen climate classification, the climate
161 is subtropical humid over the southern part of the basin, continental humid with hot summer over the
162 central part, continental humid with warm summer over the eastern and norther parts, whereas a
163 semiarid cold climate affects the western part. The average annual air temperature across the
164 watershed ranges from 4°C in the West to 6°C in the East. On average, the watershed receives about
165 900 mm/year of precipitation (77% as rainfall and 23% as snowfall), more concentrated in the eastern
166 and southern portions of the basin with respect to its northern and western part (Vose et al., 2014).

167 The river flow has a clear natural seasonality mainly controlled by spring snowmelt in the
168 mountainous areas of the basins and by heavy rainfall exceeding the soil moisture storage capacity in
169 the central and southern part of the basin (Berghuijs et al., 2016), but it is also heavily regulated by
170 the presence of about 1000 large dams (Global Reservoir and Dam Database GRanD, Lehner et al.,
171 2011) spread-out across the basin. The annual average of Mississippi river discharge at the Vicksburg

172 outlet section is equal to 17'500 m³/s (see Table 1). Given the variety of climate and topography
173 across the Mississippi River basin, it is a good candidate to test the suitability of the STREAM v1.3
174 model for river discharge and runoff simulation.

175 3. DATASETS

176 The datasets used in this study include in situ observations, satellite products and model outputs. The
177 first two datasets have been used as input data to the STREAM v1.3 model. Conversely, the model
178 outputs are used as a benchmark to validate the performance of the STREAM v1.3 model.

179 3.1 In situ Observations

180 In situ observations comprise air temperature (T_{air}) and river discharge data (Q).

181 For T_{air} data the Climate Prediction Center (CPC) Global Temperature data developed by the
182 American National Oceanic and Atmospheric Administration (NOAA) using the optimal
183 interpolation of quality-controlled gauge records of the Global Telecommunication System (GTS)
184 network (Fan et al., 2008) have been used. The dataset, downloadable at
185 (<https://psl.noaa.gov/data/gridded/data.cpc.globaltemp.html>) is available on a global regular
186 0.5°×0.5° grid, and provides daily maximum (T_{max}) and minimum (T_{min}) air temperature data from
187 1979 to present. The daily average air temperature data have been generated as the mean of T_{max} and
188 T_{min} of each day.

189 Daily Q data over the study basins have been taken from the Global Runoff Data Center (GRDC,
190 https://www.bafg.de/GRDC/EN/Home/homepage_node.html). In particular, 11 gauging stations
191 located along the main river network of the Mississippi River basin have been selected to represent
192 the spatial distribution of runoff over the basin. The location of these gauging stations along with
193 relevant characteristics (e.g., the upstream basin area, the mean annual river discharge and the
194 presence of upstream dams) are summarized in Table 1. As it can be noted, mean annual river
195 discharge ranges from 141 to 17'500 m³/s, and 3 out 11 sections are located downstream big dams
196 (Lehner et al., 2011).

197 **3.2 Satellite Products**

198 Satellite products include observations of precipitation (P), soil moisture and TWSA.

199 The satellite P dataset used in this study is the Multi-satellite Precipitation Analysis 3B42 Version 7
200 (TMPA 3B42 V7) estimate produced by the National Aeronautics and Space Administration (NASA)
201 as the $0.25^\circ \times 0.25^\circ$ quasi-global (50°N-S) gridded dataset. The TMPA 3B42 V7 is a gauged-corrected
202 satellite product, with a latency period of two months after the end of the month of record, available
203 at 3h sampling interval from 1998 to present (2020). Major details about the P dataset, downloadable
204 from <http://pmm.nasa.gov/data-access/downloads/trmm>, can be found in [Huffman et al. \(2007\)](#).

205 Soil moisture data have been taken from the European Space Agency Climate Change Initiative (ESA
206 CCI) Soil Moisture project (<https://esa-soilmoisture-cci.org/>) that provides a surface soil moisture
207 product (referred to first 2-3 centimeters of soil) continuously updated in term of spatial-temporal
208 coverage, sensors and retrieval algorithms ([Dorigo et al., 2017](#)). In this study, the daily combined
209 ESA CCI soil moisture product v4.2 is used, that is available at global scale with a grid spacing of
210 0.25° , for the period 1978-2016.

211 TWSA have been obtained from the Gravity Recovery And Climate Experiment (GRACE) satellite
212 mission. Here we employ the NASA Goddard Space Flight Center (GSFC) global mascon model,
213 i.e., Release v02.4, ([Luthcke et al. 2013](#)). It has been produced based on the mass concentration
214 (mascon) approach. The model provides surface mass densities on a monthly basis. Each monthly
215 solution represents the average of surface mass densities within the month, referenced at the middle
216 of the corresponding month. The model has been developed directly from GRACE level-1b K-Band
217 Ranging (KBR) data. It is computed and delivered as surface mass densities per patch over blocks of
218 approximately $1^\circ \times 1^\circ$ or about $12'000 \text{ km}^2$. Although the mascon size is smaller than the inherent
219 spatial resolution of GRACE, the model exhibits a relatively high spatial resolution. This is attributed
220 to a statistically optimal Wiener filtering, which uses signal and noise covariance matrices. The
221 coloured (frequency-dependent) noise characteristic of KBR data was taken in to account when

222 compiling the model, which has allowed for a reliable computation of these noise and signal
223 covariance matrices. They play a crucial role when filtering and allow to achieve a higher spatial
224 resolution compared to commonly applied GRACE filtering methods such as Gaussian smoothing
225 and/or destriping filters. GRACE data are available for the period 01 January 2003 to 15 July 2016.

226 **3.3 Model Outputs**

227 To establish the quality of the STREAM v1.3 model in runoff simulation, monthly runoff (R) data
228 obtained from the Global Runoff Reconstruction (GRUN_v1, [https://doi.org/10.3929/ethz-b-](https://doi.org/10.3929/ethz-b-000324386)
229 [000324386](https://doi.org/10.3929/ethz-b-000324386)) have been used for comparison. The GRUN dataset (Ghiggi et al., 2019) is a global
230 monthly R dataset derived through the use of a machine learning algorithm trained with in situ Q
231 observations of relatively small catchments ($<2500 \text{ km}^2$) and gridded precipitation and temperature
232 derived from the Global Soil Wetness Project Phase 3 (GSWP3) dataset (Kim et al., 2017). The
233 dataset covers the period from 1902 to 2014 and it is provided on a $0.5^\circ \times 0.5^\circ$ regular grid.

234 **4. METHOD**

235 **4.1 STREAM Model: the Concept**

236 The concept behind the STREAM v1.3 model is that river discharge is a combination of hydrological
237 responses operating at diverse time scales (Blöschl et al., 2013; Rakovec et al., 2016). In particular,
238 river discharge can be considered made up of a *slow-flow component*, produced as outflow of the
239 groundwater storage and of a *quick-flow component*, i.e. mainly related to the surface and subsurface
240 runoff components (Hu and Li, 2018).

241 While the high spatial and temporal (i.e., intermittence) variability of precipitation and the highly
242 changing land cover spatial distribution significantly impact the variability of the *quick-flow*
243 *component* (with scales ranging from hours to days and meters to kilometres depending on the basin
244 size), *slow-flow river discharge* reacts to precipitation inputs more slowly (i.e., months) as water
245 infiltrates, is stored, mixed and is eventually released in times spanning from weeks to months.

Therefore, the two components can be estimated by relying upon two different approaches that involve different types of observations. Based on that, within the STREAM v1.3 model, satellite soil moisture, precipitation and TWSA will be used for deriving river discharge and runoff estimates. The first two variables are used as proxy of the *quick-flow* river discharge component while TWSA is exploited for obtaining its complementary part, i.e., the *slow-flow river discharge* component. Firstly, we exploit the role of the soil moisture in determining the response of the catchment to the precipitation inputs, which have been soundly demonstrated in more than ten years of literature studies (see e.g., [Brocca et al., 2017](#) for a comprehensive discussion on the topic). Secondly, we consider the important role of terrestrial water storage in determining the slow-flow river discharge component as modelled in several hydrological models (e.g., [Sneeuw et al., 2014](#)).

It is worth noting that this *modus operandi*, i.e. to model the *quick-flow* and *slow-flow* discharge component separately exploring their process controls independently, has been largely applied and tested in recent and past studies, e.g., for the estimation of the flow duration curve (see e.g., [Botter et al., 2007a, b](#); [Yokoo and Sivapalan 2011](#); [Muneepeerakul et al., 2010](#); [Ghotbi et al., 2020](#)).

4.2 STREAM Model: the Laws

The STREAM v1.3 model is a conceptual hydrological model that, by using as input observation of P , soil moisture, TWSA and T_{air} data, simulates continuous R and Q time series.

The model entails three main components (Figure 1): 1) a snow module to separate precipitation into snowfall and rainfall, 2) a soil module to simulate the evolution in time t of the quick and slow runoff responses, Q_{fu} [mm] and Q_{sl} [mm], and 3) a routing module that transfers these components through the basins and the rivers for the simulation of the *quick-flow* river discharge, QF [m³/s], and the *slow-flow* river discharge, SF [m³/s] components.

The soil module is composed of two storages, S_u and S_l as illustrated in Figure 1. The upper storage receives inputs from P , released through a snow module ([Cislaghi et al., 2020](#)) as rainfall (r) or stored as snow water equivalent (SWE) within the snowpack and on the glaciers. In particular, according to

271 Cislaghi et al. (2020), *SWE* is modelled by using as input T_{air} and a degree-day coefficient, C_m , to be
 272 estimated by calibration.

273 Once separated, r input contributes to the quick runoff response while the *SWE* (like other fluxes
 274 contributing to modify the soil water content into Su) is neglected as already considered in the satellite
 275 TWSA. Therefore, the first key point of the STREAM v1.3 model is that the water content in the
 276 upper storage is directly provided by the satellite soil moisture observations and the loss processes
 277 like infiltration or evaporation do not need to be explicitly modelled to simulate the evolution in time
 278 t of soil moisture. Consequently, the quick runoff response, Qfu from the first storage can be
 279 computed following the formulation proposed by Georgakakos and Baumer (1996), as in equation
 280 (1):

$$281 \quad Qfu(t) = r(t) SWI(t, T)^\alpha \quad (1)$$

282 where:

283 - *SWI* is the Soil Water Index (Wagner et al., 1999), i.e., the root-zone soil moisture product referred
 284 to the first layer of the model (representative of the first 5-30 centimeters of soil), derived by the
 285 surface satellite soil moisture product, θ , by applying the exponential filtering approach in its
 286 recursive formulation (Albergel et al., 2009):

$$287 \quad SWI_n = SWI_{n-1} + K_n(\theta(t_n) - SWI_{n-1}) \quad (2)$$

288 with the gain K_n at the time t_n given by:

$$289 \quad K_n = \frac{K_{n-1}}{K_{n-1} + e^{\left(\frac{t_n - t_{n-1}}{T}\right)}} \quad (3)$$

290 - T [days] is a parameter, named characteristic time length, that characterizes the temporal variation
 291 of soil moisture within the root-zone profile and the gain K_n ranges between 0 and 1;

292 - $\alpha[-]$ is a coefficient linked to the non-linearity of the infiltration process and it takes into account
 293 the characteristics of the soil;

294 - for the initialization of the filter $K_1 = 1$ and $SWI_1 = \theta(t_1)$.

295 The second key point of STREAM v1.3 model concerns the estimation of the slow runoff response,
 296 Q_{sl} , from the second storage. The hypothesis here, shared also with other studies (e.g., Rakovec et al.,
 297 2016), is that the dynamic of the slow runoff component can be represented by the monthly TWSA
 298 data. Indeed, the time scale of slow runoff response is typically in the range of seasons to years and it
 299 can be assumed almost independent upon the water that is contained in that upper storage. For that, the
 300 slow runoff response Q_{sl} , from the second storage, can be computed following the formulation
 301 proposed by Famiglietti and Wood (1994), through equation (4) as follows:

$$302 \quad Q_{sl}(t) = \beta (TWSA^*(t))^m \quad (4)$$

303 where:

- 304 - $TWSA^*$ [-] is the TWSA estimated by GRACE normalized by its minimum and maximum values.
 305 The assumption behind this equation is that TWSA can be assumed as a proxy of the evolution in
 306 time, t , of the Sl , i.e., the storage of the lower storage.
- 307 - β [mm h⁻¹] and m [-] are two parameters describing the nonlinearity between slow runoff
 308 component and $TWSA^*$.

309 Note that we made the hypothesis that soil moisture and TWSA observations are independent
 310 (whereas in the reality soil moisture can be responsible both for the generation of the quick flow part
 311 (mainly) and for the slow flow contribution) given the different temporal (and spatial) scales at which
 312 the quick and slow runoff responses act.

313 The STREAM v1.3 model runs in a semi-distributed version in which the catchment is divided into
 314 s elements, each one representing either a subcatchment with outlet along the main channel or an area
 315 draining directly into the main channel. Each element is assumed homogeneous and hence constitutes
 316 a lumped system.

317 The routing module (controlled by a γ parameter) conveys the Q_{fu} and Q_{sl} response components at
 318 each element outlet (subcatchments and directly draining areas, Brocca et al., 2011) and successively

at the catchment outlet of the basin. Specifically, the quick component Q_{fu} is routed to the element outlet by the Geomorphological Instantaneous Unit Hydro-graph (GIUH, [Gupta et al., 1980](#)) for subcatchments or through a linear reservoir approach ([Nash, 1957](#)) for directly draining areas; the Q_{sl} slow component is transferred to the outlet section by a linear reservoir approach. Finally, a diffusive linear approach (controlled by the parameters C and D , i.e., Celerity and Diffusivity, [Troutman and Karlinger, 1985](#)) is applied to route the quick and slow runoff components at the outlet section of the catchment ([Brocca et al., 2011](#)). In the first case we obtain the *quick-flow* river discharge component, QF [m^3/s], and in the second case the *slow-flow* river discharge component, SF [m^3/s] (see Figure 1).

4.3 STREAM Parameters

The STREAM v1.3 model uses 8 parameters of which 5 are used in the soil module (α , T [days], β [$mm\ h^{-1}$], m , C_m) and 3 in the routing module (γ , C [$km\ h^{-1}$] and D [$km^2\ h^{-1}$]). The parameter values, determined within the feasible parameter space (See Table Appendix A for more details), are calibrated by maximizing the Kling-Gupta Efficiency index (KGE, [Gupta et al., 2009](#); [Kling et al., 2012](#), see paragraph 5.1 for more details) between observed and simulated river discharge.

5. EXPERIMENTAL DESIGN

5.1 Modelling Setup for Mississippi River Basin

The modelling setup is carried out in four steps (Figure 2):

1. *Input data collection*. Two different groups of data have to be collected to setup the model, i.e., topographic information and hydrological variables. Concerning the topographic information, the SHuttle Elevation Derivatives at multiple Scales (HydroSHED, <https://www.hydrosheds.org/>) DEM of the basin at the 3'' resolution (nearly 90 m at the equator) as well as the location of the gauging stations where the model should be calibrated/validated, are collected. Concerning the hydrological variables, gridded precipitation, T_{air} , soil moisture and TWSA are collected. In addition, in situ Q

time series for the sections where the model should be calibrated/validated as well as modelled runoff datasets are required.

2. *Sub-basin delineation.* STREAM v1.3 model is run in the semi-distributed version over the Mississippi River basin. The TopoToolbox (<https://topotoolbox.wordpress.com/>), a tool developed in Matlab by Schwanghart et al. (2010), and the DEM of the basin have been used to derive flow directions, to extract the stream network and to delineate the drainage basins over the Mississippi River basin. In particular, by considering only rivers with order greater than 3 (according to the Horton-Strahler rules, Horton, 1945; Strahler, 1952), the Mississippi watershed has been divided into 53 sub-basins as illustrated in Figure 3. Red dots in the figure indicate the location of the 11 discharge gauging stations selected for the study area.

It has to be specified that the step of sub-basin delineation could be accomplished through tools different from the TopoToolbox. For instance, it could be used the free Qgis software downloadable at <https://www.qgis.org/it/site/forusers/download.html>, following the instruction to perform the hydrological analysis as in https://docs.qgis.org/3.16/en/docs/training_manual/processing/hydro.html?highlight=hydrological%20analysis.

3. *Extraction of input data.* Precipitation, T_{air} , soil moisture and TWSA datasets data have to be extracted for each sub-basin of the study area. If characterized by different spatial/temporal resolution, these datasets need to be resampled over a common spatial grid/temporal time step prior to be used as input into the model.

To run the STREAM v1.3 model over the Mississippi river basin, input data have been resampled over the precipitation spatial grid at 0.25° resolution through a bilinear interpolation. Concerning the temporal scale, T_{air} , soil moisture and precipitation data are available at daily time step, while monthly TWSA data have been linearly interpolated at daily time step. For each of the 53 Mississippi subbasins, the resampled precipitation, soil moisture, T_{air} and TWSA data have been extracted.

368 4. *STREAM model calibration.* In situ river discharge data are used as reference data for the
369 calibration of STREAM v1.3 model. For Mississippi, the STREAM v1.3 model has been calibrated
370 over five sections as illustrated in Figure 3: the inner sections 4, 6, 9, 11 and the outlet section 10, are
371 used to calibrate the model and all sub-basins contributing to the respective sections are highlighted
372 with the same colour. This means that, for example, the sub-basins labelled as 1, 2, 5 to 15, 17, 22,
373 23, and 30 contribute to section 4, sub-basins 31, 37, 38 and 41 contribute to section 6 and so on.
374 Consequently, the sub-basins highlighted with the same colour are assigned the same model
375 parameters, i.e. the parameters that allow to reproduce the river discharge data observed at the related
376 outlet section.

377 Once calibrated, the STREAM v1.3 model has been run to provide continuous daily Q and R time
378 series, at the outlet section of each subbasin and over each grid pixel, respectively. By considering
379 the spatial/temporal availability of both in situ and satellite observations, the entire analysis period
380 covers the maximum common observation period, i.e., from 01 January 2003 to 15 July 2016 at daily
381 time scale. To establish the goodness-of-fit of the model, the simulated river discharge and runoff
382 timeseries are compared against in situ river discharge and modelled runoff data.

383 **5.2 Model Evaluation Criteria and Performance Metrics**

384 The model has been run over a 13.5-year period split into two sub periods: the first 8 years, from
385 January 2003 to December 2010, have been used to calibrate the model successively validated over
386 the remaining 5.5 years (January 2011 - July 2016).

387 In particular, three different validation schemes have been adopted to assess the robustness of the
388 STREAM v1.3 model:

- 389 1. Internal validation aimed to test the plausibility of both the model structure and the parameter
390 set in providing reliable estimates of the hydrological variables against which the model is
391 calibrated. For this purpose, a comparison between observed and simulated river discharge
392 time series on the sections used for model calibration has been carried out for both the
393 calibration and validation sub periods.

2. Cross-validation testing the goodness of the model structure and the calibrated model parameters to predict hydrological variables at locations not considered in the calibration phase. In this respect, the cross-validation has been carried out by comparing observed and simulated river discharge time series in gauged basins not considered during the calibration phase;
3. External validation aimed to test the capability of the model “*to get the right answers for the right reasons*” (Kirchner 2006). In this respect, the capability of the model to reproduce variables (e.g., fluxes or state variables) other than discharge and not considered in the calibration phase, should be tested. As runoff is a secondary product of the STREAM v1.3 model, obtained indirectly from the calibration of the river discharge (basin-integrated runoff), the comparison in terms of runoff can be considered as a further external validation of the model. Runoff, differently from discharge, cannot be directly measured. It is generally modelled through land surface or hydrological models. Its validation requires a comparison against modelled data that, however, suffer from uncertainties (Beck et al., 2017). Based on that, in this study the GRUN runoff dataset described in the section 3.3 has been used for a qualitative comparison.

5.3 Performance Metrics

To measure the goodness-of-fit between simulated and observed river discharge data three performance scores have been used:

- the relative root mean square error, RRMSE:

$$RRMSE = \frac{\sqrt{\frac{1}{n} \sum_{i=1}^n (Q_{sim_i} - Q_{obs_i})^2}}{\frac{1}{n} \sum_{i=1}^n (Q_{obs_i})} \quad (5)$$

where Q_{obs} and Q_{sim} are the observed and simulated discharge time series of length n . RRMSE values range from 0 to $+\infty$, the lower the RRMSE, the better the agreement between observed and simulated data.

- the Pearson correlation coefficient, R , measures the linear relationship between two variables:

$$R = \frac{\sum_{i=1}^n (Q_{sim_i} - \overline{Q_{sim}})(Q_{obs_i} - \overline{Q_{obs}})}{\sqrt{\sum_{i=1}^n (Q_{sim_i} - \overline{Q_{sim}})^2 (Q_{obs_i} - \overline{Q_{obs}})^2}} \quad (6)$$

where $\overline{Q_{obs}}$ and $\overline{Q_{sim}}$ represent the mean values of Q_{obs} and Q_{sim} , respectively. The values of R range between -1 and 1 ; higher values of R indicate a better agreement between observed and simulated data.

- the Kling-Gupta efficiency index (KGE, [Gupta et al., 2009](#)), which provides direct assessment of four aspects of discharge time series, namely shape, timing, water balance and variability. It is defined as follows:

$$KGE = 1 - \sqrt{(R - 1)^2 + (\delta - 1)^2 + (\varepsilon - 1)^2} \quad (7)$$

where R is the correlation coefficient, δ the relative variability and ε the bias normalized by the standard deviation between observed and simulated discharge. The KGE values range between $-\infty$ and 1 ; the higher the KGE, the better the agreement between observed and simulated data. Simulations characterized by values of KGE in the range -0.41 and 1 can be assumed as reliable; values of KGE greater than 0.5 have been assumed good with respect to their ability to reproduce observed time series ([Thiemig et al., 2013](#)).

6. RESULTS

The testing and validation of the STREAM v1.3 model is presented and discussed in this section according to the scheme illustrated in section 5.2.

6.1 Internal Validation

The performance of the STREAM v1.3 model over the calibrated river sections is illustrated in Figure 4 and summarized in Table 2. Figure 4 shows observed and simulated river discharge time series over the whole study period (2003-2016); in Table 2 the performance scores are evaluated separately for the calibration and validation sub periods. It is worth noting that the model accurately simulates the observed river discharge data and is able to give the “right answer” with good modelling performances. Score values of KGE and R over the calibration (validation) period are higher than

0.62 (0.67) and 0.75 (0.75) (resp.) for all the sections; RRMSE is lower than 46% (51%) for all the sections except for section 9, where it rises up to 71% (77%). The performances remain good even if they are evaluated over the entire study period as indicated by the scores on the top of each plot of Figure 4.

6.2 Cross-validation

The cross-validation has been carried out over the six river sections illustrated in Figure 5 not used in the calibration step. The performance scores on the top of each plot refer to the entire study periods; the scores split for calibration and validation periods are reported in Table 2. For some river sections the performance is quite low (see, e.g., river section 1, 2 and 5) whereas for others the model is able to simulate the observed discharge data quite accurately (e.g., 7 and 8). In particular, for river sections 1, 2 even if KGE reaches values equal to 0.35 and 0.40 (for the whole period), respectively, there is not a good agreement between observed and simulated river discharge and the R score is lower than 0.55 for both river sections. The worst performance is obtained over section 5, with negative KGE and low R (high RRSME). These results are certainly influenced by the presence of dams located upstream to these river sections (see Table 1): the model, not having a specific module for modelling reservoirs, is not able to accurately reproduce the dynamics of river discharge over regulated river sections. Positive KGE values are obtained over river sections 3, 7 and 8. In particular, over sections 3 (influenced by the presence of dams in section 1 and 2) and 7 (located over the Rock river, a relatively small tributary of Mississippi river, see Table 1), the STREAM v1.3 model overestimates the observed river discharge highlighting that the model parameters estimated for river section 4 and 6, respectively, are not suitable to accurately reproduce river discharge for river sections 3 and 7 (see Figure 3 and Figure 5). Conversely, the performances over river section 8, whose parameters have been set equal to the ones of river section 10, are quite high (KGE equal to 0.71, 0.80 and 0.77 for the entire, the calibration and the validation period, respectively; R equal to 0.83, 0.84 and 0.84 for the entire, calibration and validation periods, respectively).

468 Although it is expected that the performances of STREAM v1.3 model, as any hydrological model
469 calibrated against observed data, can decrease over the gauging sections not used for the calibration,
470 the findings obtained above raises doubts about the robustness of model parameters and whether it is
471 actually possible to transfer model parameters from one river section to another with different
472 interbasin characteristics. A more in-depth investigation about the model calibration procedure and
473 the regionalization of the model parameters will be carried out in future studies.

474 **6.3 External Validation**

475 For the external validation, the monthly runoff time series provided by the GRUN datasets have been
476 compared against the ones computed by the STREAM v1.3 model. For that, STREAM daily runoff
477 time series have been aggregated at monthly scale and re-gridded at the same spatial resolution of the
478 GRUN dataset (0.5°). The comparison is illustrated in Figure 6 for the common period 2003–2014.
479 Although the two datasets consider different precipitation inputs, the two models agree in identifying
480 two distinct zones in terms of runoff, i.e., the western dry and the eastern wet area. This two distinct
481 zones can be clearly identified also in the GSWP3 and TMPA 3B42 V7 precipitation maps (not shown
482 here) used as input in GRUN and STREAM v1.3, respectively, stressing that STREAM runoff output
483 is correctly driven by the input data. However, likely due to the calibration procedure, the STREAM
484 runoff map appears patchier with respect to GRUN and discontinuities along the sub-basin boundaries
485 (identified in Figure 3) can be noted. This should be ascribed to the automatic calibration procedure
486 of the model that, differently from other calibration techniques (e. g., regionalization procedures),
487 does not consider the basin physical attributes like soil, vegetation, and geological properties that
488 govern spatial dynamics of hydrological processes. This calibration procedure can generate sharp
489 discontinuities even for neighbouring subcatchments individually calibrated. It leads to
490 discontinuities in model parameter values and consequently in the simulated hydrological variable
491 (runoff).

492 7. DISCUSSION

493 In the previous sections, the ability of the STREAM v1.3 model to accurately simulate river discharge
494 and runoff time series has been presented. In particular, Figures 4, 5 and 6 demonstrate that satellite
495 observations of precipitation, soil moisture and terrestrial water storage anomalies can provide
496 accurate daily river discharge estimates for near-natural large basins (absence of upstream dams), and
497 for basins with draining area lower than 160'000 km² (see section 7), i.e., at spatial/temporal
498 resolution lower than the ones of the TWSA input data (monthly, 160'000 km²). This is an important
499 result of the study as it demonstrates, on one hand, that the model structure is appropriate with respect
500 to the data used as input and, on the other hand, the great value of information contained into TWSA
501 data that, even if characterized by limited spatial/temporal resolution, can be used to simulate runoff
502 and river discharge at basin scale. This finding has been also confirmed by a preliminary sensitivity
503 analysis in which the STREAM v1.3 model has been run with different hydrological inputs of
504 precipitation, soil moisture and total water storage anomaly (not shown here for brevity). In particular,
505 by running the STREAM v1.3 model with different input configurations (e.g., by using TMPA 3B42
506 V7 or Climate Prediction Center (CPC) data for precipitation, ESA CCI or Advanced SCATterometer
507 (ASCAT) data for soil moisture, TWSA or soil moisture data to simulate the slow-flow river
508 discharge component), we found that STREAM results are more sensitive to soil moisture data rather
509 than to precipitation input. In addition, by running STREAM v1.3 model with soil moisture data as
510 input to simulate the slow-flow river discharge component (i.e. without using TWSA data) we found
511 a deterioration of the model results.

512 Hereinafter, the strengths and the main limitations of the STREAM v1.3 model are discussed.

513 Among the strengths of the STREAM v1.3 model it is worth highlighting:

514 1. **Remote sensing-based conceptual hydrological model.** Discharge and runoff estimates are
515 obtained through a remote sensing-based conceptual hydrological model, simpler than classical
516 hydrological models or LSMs. In particular, discharge and runoff estimates are obtained by exploiting

517 as much as possible satellite observations and by keeping the modelling component at a minimum.
518 The knowledge of the key mechanisms and processes that act in the formation of runoff, like the role
519 of the soil moisture in determining the response of the catchment to precipitation, played a major role
520 in the definition of the model structure. Being an observational-based approach, the STREAM v1.3
521 model presents two main advantages: 1) possibility to directly ingest observations (soil moisture and
522 terrestrial water storage data) into the model structure, allowing to take implicitly into account some
523 processes, mainly human-driven (e.g., irrigation, change in the land use), which might have a large
524 impact on the hydrological cycle and hence on total runoff; 2) the independence with respect to
525 existing large scale hydrological models such as, e.g., the evapotranspiration is not explicitly
526 modelled.

527 **2. Simplicity.** The STREAM v1.3 model structure: 1) limits the input data required (only
528 precipitation, T_{air} , soil moisture and TWSA data are needed as input; LSM/GHMs require many
529 additional inputs such as wind speed, shortwave and longwave radiation, pressure and relative
530 humidity); 2) limits and simplifies the processes to be modelled for runoff/discharge simulation.
531 Processes like evapotranspiration, infiltration or percolation, are not modelled therefore avoiding the
532 need of using sophisticated and highly parameterized equations (e.g., Penman-Monteith for
533 evapotranspiration, Allen et al.,1998, Richard equation for infiltration, Richard, 1931); 3) limits the
534 number of parameters (only 8 parameters have to be calibrated) thus simplifying the calibration
535 procedure and potentially reduce the model uncertainties related to the estimation of parameter
536 values.

537 **3. Versatility.** The STREAM v1.3 model is a versatile model suitable for daily runoff and discharge
538 estimation over sub-basins with different physiographic characteristics. The results obtained in this
539 study clearly indicate the potential of this approach to be extended at the global scale. Moreover, the
540 model can be easily adapted to ingest input data with spatial/temporal resolution different from the
541 one tested in this study (0.25°/daily). For instance, satellite missions with higher space/time

542 resolution, or near real time satellite products could be considered. As an example, the Next
543 Generation Gravity Mission design studies all encompass double-pair scenarios, which would greatly
544 improve upon the current spatial resolution of single-pair missions like GRACE and GRACE-FO (>
545 100'000 km²).

546 **4. Computationally inexpensive.** Due to its simplicity and the limited number of parameters to be
547 calibrated, the computational effort for the STREAM v1.3 model is very limited.

548

549 However, some limitations have to be acknowledged for the current version of the STREAM v1.3
550 model:

551 **1. Presence of reservoir, diversion, dams or flood plain.** As the STREAM v1.3 model does not
552 explicitly consider the presence of discontinuity elements along the river network (e. g, reservoir,
553 dam or floodplain), discharge estimates obtained for sections located downstream of such elements
554 might be inaccurate (see, e.g., river sections 1 and 2 in Figure 5).

555 **2. Need of in situ data for model calibration and robustness of model parameters.** As discussed
556 in the results section, parameter values of the STREAM v1.3 model are set through an automatic
557 calibration procedure aimed at minimizing the differences between simulated and observed river
558 discharge. The main drawback of this parameterization technique is that the models parameterized
559 with this technique may exhibit (1) poor predictability of state variables and fluxes at locations and
560 periods not considered in the calibration, and (2) sharp discontinuities along sub-basin boundaries in
561 state flux, and parameter fields (e.g., Merz and Blöschl, 2004).

562 To overcome these issues, several regionalization procedures, as for instance summarized in Cislaghi
563 et al. (2020), could be conveniently applied to transfer model parameters from hydrologically similar
564 catchments to a catchment of interest. In particular, the regionalization of model parameters could
565 allow to: i) estimate discharge and runoff time series over ungauged basins overcoming the need of
566 discharge data recorded from in-situ networks; ii) estimate the model parameter values through a
567 physically consistent approach, linking them to the characteristics of the basins; iii) solve the problem

568 of discontinuities in the model parameters, avoiding to obtain patchy unrealistic runoff maps.
569 However, this aspect is beyond the paper purpose and it will conveniently addressed in future works.

570 **8. CONCLUSIONS**

571 This study presents a new conceptual hydrological model, STREAM v1.3, for runoff and river
572 discharge estimation. By using as input satellite data of precipitation, soil moisture and terrestrial
573 water storage anomalies, the model has been able to provide accurate daily river discharge and runoff
574 estimates at the outlet river section and the inner river sections and over a $0.25^{\circ} \times 0.25^{\circ}$ spatial grid of
575 the Mississippi river basin. In particular, the model is suitable to reproduce:

- 576 1. river discharge time series over the calibrated river section with good performances both in
577 calibration and validation periods;
- 578 2. river discharge time series over river sections not used for calibration and not located downstream
579 dams or reservoirs;
- 580 3. runoff time series with a quite good agreement with respect to the well-established GRUN
581 observational-based dataset used for comparison.

582 The integration of observations of soil moisture, precipitation and terrestrial water storage anomalies
583 is a first alternative method for river discharge and runoff estimation with respect to classical methods
584 based on the use of TWSA-only (suitable for river basins larger than $160'000 \text{ km}^2$, monthly time
585 scale) or on classical LSMs (Cai et al., 2014).

586 Moreover, although simple, the model has demonstrated a great potential to be easily applied over
587 subbasins with different climatic and topographic characteristics, suggesting also the possibility to
588 extend its application to other basins. In particular, the analysis over basins with high human impact,
589 where the knowledge of the hydrological cycle and the river discharge monitoring is very important,
590 deserves special attention. Indeed, as the STREAM v1.3 model is directly ingesting observations of
591 soil moisture and terrestrial water storage data, it allows the modeller to neglect processes that are
592 implicitly accounted for in the input data. Therefore, human-driven processes (e.g., irrigation, land

593 use change), that are typically very difficult to simulate due to missing information and might have a
594 large impact on the hydrological cycle, hence on total runoff, could be implicitly modelled. The
595 application of the STREAM v1.3 model on a larger number of basins with different climatic-
596 physiographic characteristics (e.g., including more arid basins, snow-dominated, lots of topography,
597 heavily managed) will be object of future studies and it will allow to investigate the possibility to
598 regionalize the model parameters and overcome the limitations of the automatic calibration procedure
599 highlighted in the discussion section.

600 **AUTHOR CONTRIBUTION**

601 S.C. performed the analysis and wrote the manuscript. G.G. collected the data and helped in
602 performing the analysis; C.M, L.B., A.T., N.S., H.H.F., C.M., M.R. and J.B. contributed to the
603 supervision of the work. All authors discussed the results and contributed to the final manuscript.

604 **CODE AVAILABILITY**

605 The STREAM model version 1.3, with a short user manual, is freely downloadable in Zenodo
606 (<https://zenodo.org/record/4744984>, doi: 10.5281/zenodo.4744984). The STREAM v1.3 model code
607 is distributed through M language files, but it could be run with different interpreters of M language,
608 like the GNU Octave (freely downloadable here <https://www.gnu.org/software/octave/download>).

609 **DATA AVAILABILITY**

610 All data and codes used in the study are freely available online. Air temperature data are available at
611 <https://psl.noaa.gov/data/gridded/data.cpc.globaltemp.html> (last access 25/11/202). In situ river
612 discharge data have been taken from the Global Runoff Data Center (GRDC,
613 https://www.bafg.de/GRDC/EN/Home/homepage_node.html (last access 25/11/202). Precipitation
614 and soil moisture data are available from <http://pmm.nasa.gov/data-access/downloads/trmm> and
615 <https://esa-soilmoisture-cci.org/>, respectively.

616 **COMPETING INTERESTS**

617 The authors declare that they have no conflict of interest.

618 **ACKNOWLEDGMENTS**

619 The authors wish to thank the Global Runoff Data Centre (GRDC) for providing most of the
620 streamflow data throughout Europe. The authors gratefully acknowledge support from ESA through
621 the STREAM Project (EO Science for Society element Permanent Open Call contract n°
622 4000126745/19/I-NB).

623

624 REFERENCE

- 625 Albergel, C., Rüdiger, C., Carrer, D., Calvet, J. C., Fritz, N., Naeimi, V., Bartsch, Z., & Hasenauer, S. (2009). An
626 evaluation of ASCAT surface soil moisture products with in-situ observations in southwestern France. *Hydrology and*
627 *Earth System Sciences*, 13, 115–124, doi:10.5194/hess-13-115-2009.
- 628 Allen RG, Pereira LS, Raes D, Smith M (1998) Crop evapotranspiration — guidelines for computing crop water
629 requirements. FAO Irrigation & Drainage Paper 56. FAO, Rome.
- 630 Balsamo, G., A. Beljaars, K. Scipal, P. Viterbo, B. vanden Hurk, M. Hirschi, and A. K. Betts (2009). A revised hydrology
631 for the ECMWF model: Verification from field site to terrestrial water storage and impact in the integrated forecast
632 system, *J. Hydrometeorol.*, 10(3), 623–643, doi:10.1175/2008JHM1068.1.
- 633 Barbarossa, V., Huijbregts, M. A., Beusen, A. H., Beck, H. E., King, H., & Schipper, A. M. (2018). FLO1K, global maps
634 of mean, maximum and minimum annual streamflow at 1 km resolution from 1960 through 2015. *Scientific data*, 5,
635 180052.
- 636 Beck, H. E., van Dijk, A. I., de Roo, A., Dutra, E., Fink, G., Orth, R., & Schellekens, J. (2017). Global evaluation of
637 runoff from ten state-of-the-art hydrological models. *Hydrology and Earth System Sciences*, 21(6), 2881-2903. doi;
638 doi.org/10.5194/hess-21-2881-2017.
- 639 Berghuijs, W. R., Woods, R. A., Hutton, C. J., and Sivapalan, M. (2016). Dominant flood generating mechanisms across
640 the United States, *Geophys. Res. Lett.*, 43, 4382–4390, <https://doi.org/10.1002/2016GL068070>.
- 641 Berthet, L., Andréassian, V., Perrin, C., & Javelle, P. (2009). How crucial is it to account for the antecedent moisture
642 conditions in flood forecasting? Comparison of event-based and continuous approaches on 178 catchments.
643 *Hydrology and Earth System Sciences*, 13(6), 819-831.
- 644 Blöschl, G., Sivapalan, M., Wagener, T., Viglione, A., & Savenije, H. H. G. (Eds.) (2013). *Runoff predictions in ungauged*
645 *basins: A synthesis across processes, places and scales*. Cambridge: Cambridge University Press.
- 646 Botter, G., Peratoner, F., Porporato, A., Rodriguez-Iturbe, I., and Rinaldo, A. (2007b). Signatures of large-scale soil
647 moisture dynamics on streamflow statistics across U.S. Climate regimes, *Water Resour. Res.*, 43, W11413,
648 doi:10.1029/2007WR006162.
- 649 Botter, G., Porporato, A., Daly, E., Rodriguez-Iturbe, I., and Rinaldo, A. (2007a). Probabilistic characterization of base
650 flows in river basins: Roles of soil, vegetation, and geomorphology, *Water Resour. Res.*, 43,
651 W06404, doi:10.1029/2006WR005397.
- 652 Brocca, L., Melone, F., Moramarco, T. (2008). On the estimation of antecedent wetness conditions in rainfall-runoff
653 modelling. *Hydrological Processes*, 22 (5), 629-642, doi:10.1002/hyp.6629. <http://dx.doi.org/10.1002/hyp.6629>.
- 654 Brocca, L., Melone, F., Moramarco, T., & Morbidelli, R. (2009). Antecedent wetness conditions based on ERS
655 scatterometer data. *Journal of Hydrology*, 364(1-2), 73-87
- 656 Brocca, L., Melone, F., & Moramarco, T. (2011). Distributed rainfall-runoff modelling for flood frequency estimation
657 and flood forecasting. *Hydrological processes*, 25(18), 2801-2813.
- 658 Brocca, L., Ciabatta, L., Massari, C., Camici, S., & Tarpanelli, A. (2017). Soil moisture for hydrological applications:
659 open questions and new opportunities. *Water*, 9(2), 140.
- 660 Cai, X., Yang, Z. L., David, C. H., Niu, G. Y., & Rodell, M. (2014). Hydrological evaluation of the Noah-MP land surface
661 model for the Mississippi River Basin. *Journal of Geophysical Research: Atmospheres*, 119(1), 23-38.
- 662 Cislighi, A., Masseroni, D., Massari, C., Camici, S., & Brocca, L. (2020). Combining a rainfall–runoff model and a
663 regionalization approach for flood and water resource assessment in the western Po Valley, Italy. *Hydrological*
664 *Sciences Journal*, 65(3), 348-370.
- 665 Crochemore, L., Isberg, K., Pimentel, R., Pineda, L., Hasan, A., & Arheimer, B. (2020). Lessons learnt from checking
666 the quality of openly accessible river flow data worldwide. *Hydrological Sciences Journal*, 65(5), 699-711
- 667 Crow, W. T., Bindlish, R., & Jackson, T. J. (2005). The added value of spaceborne passive microwave soil moisture
668 retrievals for forecasting rainfall-runoff partitioning. *Geophysical Research Letters*, 32(18).

669 Döll, P., F.Kaspar, and B.Lehner (2003), A global hydrological model for deriving water availability indicators: Model
670 tuning and validation, *J. Hydrol.*, 270(1–2), 105–134, doi:10.1016/S0022-1694(02)00283-4.

671 Dorigo, W., Wagner, W., Albergel, C., Albrecht, F., Balsamo, G., Brocca, L., Chung, D., Ertl, M., Forkel, M., Gruber, A.,
672 Haas, D., Hamer, P. Hirschi, M., Ikonen, J., de Jeu, R., Kidd, R., Lahoz, W., Liu, Y.Y., Miralles, D., Mistelbauer, T.,
673 Nicolai-Shaw, N., Parinussa, R., Pratola, C., Reimer, C., van der Schalie, R., Seneviratne, S.I., Smolander, T.,
674 Lecomte, P. (2017). ESA CCI Soil Moisture for improved Earth system understanding: state-of-the art and future
675 directions. *Remote Sensing of Environment*, 203, 185–215.

676 Entekhabi, D., Njoku, E. G., O'Neill, P. E., Kellogg, K. H., Crow, W. T., Edelstein, W. N., ... & Van Zyl, J. (2010). The
677 soil moisture active passive (SMAP) mission. *Proceedings of the IEEE*, 98(5), 704–716. doi:
678 10.1109/JPROC.2010.2043918.

679 Famiglietti, J.S., Wood, E. F. (1994). Multiscale modeling of spatially variable water and energy balance processes. *Water*
680 *Resour. Res.*, 30, 3061–3078.

681 Famiglietti, J. S., & Rodell, M. (2013). Water in the balance. *Science*, 340(6138), 1300–1301.

682 Fan, Y. & Van den Dool, H. A (2008). Global monthly land surface air temperature analysis for 1948–present. *Journal of*
683 *Geophysical Research: Atmospheres* 113, D01103.

684 Fekete, B. M., Looser, U., Pietroniro, A., and Robarts, R. D. (2012). Rationale for monitoring discharge on the ground,
685 *J. Hydrometeorol.*, 13, 1977–1986.

686 Georgakakos KP, Baumer OW. (1996). Measurement and utilization of onsite soil moisture data. *Journal of Hydrology*
687 184: 131–152.

688 Ghiggi, G., Humphrey, V., Seneviratne, S. I., & Gudmundsson, L. (2019). GRUN: an observation-based global gridded
689 runoff dataset from 1902 to 2014. *Earth System Science Data*, 11(4), 1655–1674.

690 Ghotbi, S., Wang, D., Singh, A., Blöschl, G., & Sivapalan, M. (2020). A New Framework for Exploring Process Controls
691 of Flow Duration Curves. *Water Resources Research*, 56(1), e2019WR026083.

692 Gudmundsson, L., & Seneviratne, S. I. (2016). Observation-based gridded runoff estimates for Europe (E-RUN version
693 1.1). *Earth System Science Data*, 8(2), 279–295.

694 Gudmundsson, L., Wagener, T., Tallaksen, L. M., & Engeland, K. (2012a). Evaluation of nine large-scale hydrological
695 models with respect to the seasonal runoff climatology in Europe. *Water Resources Research*, 48(11).

696 Gudmundsson, L., Tallaksen, L. M., Stahl, K., Clark, D. B., Du-mont, E., Hagemann, S., Bertrand, N., Gerten, D., Heinke,
697 J., Hanasaki, N., Voss, F., and Koirala, S. (2012b). Comparing Large-Scale Hydrological Model Simulations to
698 Observed Runoff Percentiles in Europe, *J. Hydrometeorol.*, 13, 604–62.

699 Gupta VK, Waymire E, Wang CT. (1980). A representation of an instantaneous unit hydrograph from geomorphology.
700 *Water Resources Research* 16: 855–862, doi: 10.1029/WR016i005p00855.

701 Gupta, H. V., Kling, H., Yilmaz, K. K., & Martinez, G. F. (2009). Decomposition of the mean squared error and NSE
702 performance criteria: Implications for improving hydrological modelling. *Journal of Hydrology*, 377(1–2), 80–91.

703 Haddeland, I., Heinke, J., Voß, F., Eisner, S., Chen, C., Hagemann, S., & Ludwig, F. (2012). Effects of climate model
704 radiation, humidity and wind estimates on hydrological simulations. *Hydrology and Earth System Sciences*, 16(2),
705 305–318.

706 Hastie, T., Tibshirani, R., and Friedman, J. H. (2009). *The Elements of Statistical Learning – Data Mining, Inference, and*
707 *Prediction*, Second Edition, Springer Series in Statistics, Springer, New York, 2nd Edn., available at: [http://www-](http://www-stat.stanford.edu/~tibs/ElemStatLearn/)
708 [stat.stanford.edu/~tibs/ElemStatLearn/](http://www-stat.stanford.edu/~tibs/ElemStatLearn/) (last access: 5 July 2016).

709 Hong, Y., Adler, R. F., Hossain, F., Curtis, S., & Huffman, G. J. (2007). A first approach to global runoff simulation
710 using satellite rainfall estimation. *Water Resources Research*, 43(8).

711 Horton, R. E. (1945). Hydrological approach to quantitative morphology. *Geol. Soc. Am. Bull*, 56, 275–370.

712 Houborg, R., Rodell, M., Li, B., Reichle, R., & Zaitchik, B. F. (2012). Drought indicators based on model-assimilated
713 Gravity Recovery and Climate Experiment (GRACE) terrestrial water storage observations. *Water Resources*
714 *Research*, 48(7).

715 Hu GR., Li XY. (2018). Subsurface Flow. In: Li X., Vereecken H. (eds) Observation and Measurement. Ecohydrology.
 716 Springer, Berlin, Heidelberg. https://doi.org/10.1007/978-3-662-47871-4_9-1

717 Huffman, G. J., R. F. Adler, D. T. Bolvin, G. J. Gu, E. J. Nelkin, K. P. Bowman, Y. Hong, E. F. Stocker, and D. B. Wolff.
 718 (2007). The TRMM Multisatellite Precipitation Analysis (TMPA): Quasi-Global, Multiyear, Combined-Sensor
 719 Precipitation Estimates at Fine Scales. *Journal of Hydrometeorology* 8 (1): 38–55. doi:10.1175/jhm560.1.

720 Huffman, G. J., Stocker, E. F., Bolvin, D. T., Nelkin, E. J., & Adler, R. F. (2014). TRMM Version 7 3B42 and 3B43 Data
 721 Sets. NASA/GSFC, Greenbelt, MD.

722 Huffman, G. J., Bolvin, D. T., Braithwaite D., Hsu K., Joyce R. , Kidd C., Nelkin Eric J., Sorooshian S., Tan J., Xie P.
 723 (2019). NASA Global Precipitation Measurement (GPM) Integrated Multi-satellitE Retrievals for GPM (IMERG).
 724 https://docserver.gesdisc.eosdis.nasa.gov/public/project/GPM/IMERG_ATBD_V06.pdf.

725 Kim, H., Watanabe, S., Chang, E. C., Yoshimura, K., Hirabayashi, J., Famiglietti, J., and Oki, T. (2017). Global Soil
 726 Wetness Project Phase 3 Atmospheric Boundary Conditions (Experiment 1) [Data set], Data Integration and Analysis
 727 System (DIAS), <https://doi.org/10.20783/DIAS.501>.

728 Kirchner, J. W. (2006). Getting the right answers for the right reasons: Linking measurements, analyses, and models to
 729 advance the science of hydrology. *Water Resources Research*, 42(3).

730 Kling, H., Fuchs, M., & Paulin, M. (2012). Runoff conditions in the upper Danube basin under an ensemble of climate
 731 change scenarios. *Journal of Hydrology*, 424, 264–277, doi: 10.1016/j.jhydrol.2012.01.011.

732 Landerer, F. W., & Swenson, S. C. (2012). Accuracy of scaled GRACE terrestrial water storage estimates. *Water*
 733 *resources research*, 48(4).

734 Lehner, B., C. Reidy Liermann, C. Revenga, C. Vörösmarty, B. Fekete, P. Crouzet, P. Döll, M. Endejan, K. Frenken, J.
 735 Magome, C. Nilsson, J.C. Robertson, R. Rodel, N. Sindorf, and D. Wisser. 2011. High-resolution mapping of the
 736 world's reservoirs and dams for sustainable river-flow management. *Frontiers in Ecology and the Environment* 9 (9):
 737 494–502.

738 Long, D., Longuevergne, L., & Scanlon, B. R. (2014). Uncertainty in evapotranspiration from land surface modeling,
 739 remote sensing, and GRACE satellites. *Water Resources Research*, 50(2), 1131–1151.

740 Lorenz, C., H. Kunstmann, B. Devaraju, M. J. Tourian, N. Sneeuw, and J. Riegger (2014). Large-Scale Runoff from
 741 Landmasses: A Global Assessment of the Closure of the Hydrological and Atmospheric Water Balances. *J.*
 742 *Hydrometeor.*, 15, 2111–2139, doi:10.1175/JHM-D-13-0157.1.

743 Luthcke, S.B., Sabaka, T.J., Loomis, B.D., Arendt, A.A., McCarthy, J.J., Camp, J. (2013) Antarctica, Greenland and Gulf
 744 of Alaska land-ice evolution from an iterated GRACE global mascon solution, *Journal of Glaciology*, Vol. 59, No.
 745 216, 2013 doi:10.3189/2013JoG12J147.

746 Massari, C., Brocca, L., Tarpanelli, A., Hong, Y., Crow, W., Ciabatta, L., Camici, S., Barbetta, S., Moramarco, T. (2016).
 747 Global surface runoff estimation in near real time by using SMAP and GPM, poster at SMAP conference.

748 Massari, C., Brocca, L., Barbetta, S., Papathanasiou, C., Mimikou, M., & Moramarco, T. (2014). Using globally available
 749 soil moisture indicators for flood modelling in Mediterranean catchments. *Hydrology and Earth System Sciences*,
 750 18(2), 839.

751 Merz, R., & Blöschl, G. (2009). A regional analysis of event runoff coefficients with respect to climate and catchment
 752 characteristics in Austria. *Water Resources Research*, 45(1).

753 Mueller Schmied, H., Adam, L., Eisner, S., Fink, G., Flörke, M., Kim, H., ... & Song, Q. (2016). Variations of global and
 754 continental water balance components as impacted by climate forcing uncertainty and human water use. *Hydrology*
 755 *and Earth System Sciences*, 20(7), 2877–2898.

756 Muneeppeerakul, R., Azale, S., Botter, G., Rinaldo, A., & Rodriguez-Iturbe, I. (2010). Daily streamflow analysis based
 757 on a two-scaled gamma pulse model. *Water Resources Research*, 46(11).

758 Nash, J. E. (1957). The form of the instantaneous unit hydrograph, IASH publication no. 45, 3–4, 114–121.

759 Natural Resources Conservation Service (NRCS) (1986), Urban hydrology for small watersheds, Tech. Release 55, 2nd
 760 ed., U.S. Dep. of Agric., Washington, D. C. (available at [ftp://ftp.wcc.nrcs.usda.gov/downloads/](ftp://ftp.wcc.nrcs.usda.gov/downloads/hydrology_hydraulics/tr55/tr55.pdf)
 761 [hydrology_hydraulics/tr55/tr55.pdf](ftp://ftp.wcc.nrcs.usda.gov/downloads/hydrology_hydraulics/tr55/tr55.pdf))

Orth, R., & Seneviratne, S. I. (2015). Introduction of a simple-model-based land surface dataset for Europe. *Environmental Research Letters*, 10(4), 044012.

Pellet, V., Aires, F., Munier, S., Fernández Prieto, D., Jordá, G., Dorigo, W. A., ... & Brocca, L. (2019). Integrating multiple satellite observations into a coherent dataset to monitor the full water cycle—application to the Mediterranean region. *Hydrology and Earth System Sciences*, 23(1), 465-491.

Prudhomme, C., Giuntoli, I., Robinson, E. L., Clark, D. B., Arnell, N. W., Dankers, R., ... & Hagemann, S. (2014). Hydrological droughts in the 21st century, hotspots and uncertainties from a global multimodel ensemble experiment. *Proceedings of the National Academy of Sciences*, 111(9), 3262-3267.

Rakovec, O., Kumar, R., Attinger, S., & Samaniego, L. (2016). Improving the realism of hydrologic model functioning through multivariate parameter estimation. *Water Resources Research*, 52(10), 7779-7792.

Richards, L.A. (1931). Capillary conduction of liquids through porous mediums. *Physics*. 1 (5): 318–333. Bibcode:1931Physi.1.318R. doi:10.1063/1.1745010.

Riegger, J., and M. J. Tourian (2014), Characterization of runoff-storage relationships by satellite gravimetry and remote sensing, *Water Resour. Res.*, 50, 3444–3466, doi:10.1002/2013WR013847.

Rodell, M., Beaudoin, H. K., L’Ecuyer, T. S., Olson, W. S., Famiglietti, J. S., Houser, P. R., Adler, R., Bosilovich, M. G., Clayson, C. A., Chambers, D., Clark, E., Fetzer, E. J., Gao, X., Gu, G., Hilburn, K., Huffman, G. J., Lettenmaier, D. P., Liu, W. T., Robertson, F. R., Schlosser, C. A., Sheffield, J. and Wood, E. F. (2015). The observed state of the water cycle in the early 15twenty-first century, *J. Clim.*, 28(21), 8289–8318, doi:10.1175/JCLI-D-14-00555.1.

Schellekens, J., Dutra, E., Martínez-de la Torre, A., Balsamo, G., van Dijk, A., Sperna Weiland, F., Minvielle, M., Calvet, J.-C., Decharme, B., Eisner, S., Fink, G., Flörke, M., Peßenteiner, S., van Beek, R., Polcher, J., Beck, H., Orth, R., Calton, B., Burke, S., Dorigo, W., and Weedon, G. P. (2017). A global water resources ensemble of hydrological models: the earth2Observe Tier-1 dataset, *Earth Syst. Sci. Data*, 9, 389–413, <https://doi.org/10.5194/essd-9-389-2017>.

Schwanghart, W., & Kuhn, N. J. (2010). TopoToolbox: A set of Matlab functions for topographic analysis. *Environmental Modelling & Software*, 25(6), 770-781.

Seneviratne, S. I., Corti, T., Davin, E. L., Hirschi, M., Jaeger, E. B., Lehner, I., ... & Teuling, A. J. (2010). Investigating soil moisture–climate interactions in a changing climate: A review. *Earth-Science Reviews*, 99(3-4), 125-161.

Sneeuw, N., Lorenz, C., Devaraju, B., Tourian, M. J., Riegger, J., Kunstmann, H., & Bárdossy, A. (2014). Estimating runoff using hydro-geodetic approaches. *Surveys in Geophysics*, 35(6), 1333-1359.

Solomatine, D. P., & Ostfeld, A. (2008). Data-driven modelling: some past experiences and new approaches. *Journal of hydroinformatics*, 10(1), 3-22.

Strahler, A. N. (1952). Hypsometric (area-altitude) analysis of erosional topography. *Geological Society of America Bulletin*, 63(11), 1117-1142.

Tapley, B.D., Watkins, M.M., Flechtner, F. et al. (2019). Contributions of GRACE to understanding climate change. *Nat. Clim. Chang.* 9, 358–369, doi:10.1038/s41558-019-0456-2.

Thiemig, V., Rojas, R., Zambrano-Bigiarini, M., & De Roo, A. (2013). Hydrological evaluation of satellite rainfall estimates over the Volta and Baro-Akobo Basin. *Journal of Hydrology*, 499, 324-338.

Tourian, M. J., Reager, J. T., & Sneeuw, N. (2018). The total drainable water storage of the Amazon river basin: A first estimate using GRACE. *Water Resources Research*, 54. <https://doi.org/10.1029/2017WR021674>.

Tramblay, Y., Bouvier, C., Martin, C., Didon-Lescot, J. F., Todorovik, D., & Domergue, J. M. (2010). Assessment of initial soil moisture conditions for event-based rainfall–runoff modelling. *Journal of Hydrology*, 387(3-4), 176-187.

Troutman, B. M., Karlinger, M.B. (1985). Unit hydrograph approximation assuming linear flow through topologically random channel networks. *Water Resources Research*, 21: 743 – 754, doi: 10.1029/WR021i005p00743.

Vose, R.S., Applequist, S., Durre, I., Menne, M.J., Williams, C.N., Fenimore, C., Gleason, K., & Arndt, D. (2014). Improved Historical Temperature and Precipitation Time Series For U.S. Climate Divisions. *Journal of Applied Meteorology and Climatology*, 53(May), 1232–1251. DOI: 10.1175/JAMC-D-13-0248.1

Vörösmarty C. J., and Coauthors (2002). Global water data: A newly endangered species. *Eos, Trans. Amer. Geophys. Union*, 82, 54.

809 Wagner, W., Blöschl, G., Pampaloni, P., Calvet, J. C., Bizzarri, B., Wigneron, J. P., & Kerr, Y. (2007). Operational
810 readiness of microwave remote sensing of soil moisture for hydrologic applications. *Hydrology Research*, 38(1), 1-
811 20.

812 Wagner, W., Lemoine, G., & Rott, H. (1999). A method for estimating soil moisture from ERS scatterometer and soil
813 data. *Remote Sensing of Environment*, 70, 191–207, doi:10.1016/S0034-4257(99)00036-X.

814 Wisser, D., Fekete, B. M., Vörösmarty, C. J., and Schumann, A. H. (2010). Reconstructing 20th century global
815 hydrography: a contribution to the Global Terrestrial Network- Hydrology (GTN-H), *Hydrol.Earth Syst. Sci.*, 14, 1–
816 24, doi:10.5194/hess-14-1-2010.

817 Yokoo, Y., & Sivapalan, M. (2011). Towards reconstruction of the flow duration curve: Development of a conceptual
818 framework with a physical basis. *Hydrology and Earth System Sciences*, 15(9), 2805–2819.
819 <https://doi.org/10.5194/hess-15-2805-2011>.

820 Zhang, Y., Pan, M., Sheffield, J., Siemann, A. L., Fisher, C. K., Liang, M., ... & Zhou, T. (2018). A Climate Data Record
821 (CDR) for the global terrestrial water budget: 1984–2010. *Hydrology and Earth System Sciences (Online)*, 22(PNNL-
822 SA-129750).

823

824 Table 1. Location of gauging stations over the Mississippi basins and upstream contributing area.
825 Bold text is used to indicate stations where the STREAM v1.3 model has been calibrated.

#	River	Station name	Latitude (°)	Longitude (°)	Upstream area (km ²)	Mean annual river discharge (m ³ /s)	Presence of dam
1	Missouri	Bismarck, ND	-100.82	46.81	481'232	633	Garrison dam
2	Missouri	Omaha, NE	-95.92	41.26	814'371	914	Gavins Point Dam
3	Missouri	Kansas City, MO	-94.59	39.11	1'229'427	1499	---
4	Missouri	Hermann, MO	-91.44	38.71	1'330'000	2326	---
5	Kansas	Wamego, KS	-96.30	39.20	143'054	141	Kanopolis
6	Mississippi	Keokuk, IA	-91.37	40.39	282'559	1948	---
7	Rock	Near Joslin, IL	-90.18	41.56	23'835	199	---
8	Mississippi	Chester, IL	-89.84	37.90	1'776'221	6018	---
9	Arkansas	Murray Dam Near Little Rock, AR	-92.36	34.79	408'068	1249	---
10	Mississippi	Vicksburg, MS	-90.91	32.32	2'866'590	17487	---
11	Ohio	Metropolis, ILL.	-88.74	37.15	496'134	7931	---

828 Table 2. Performance scores obtained over the Mississippi river sections during the calibration and
829 validation periods.

#	CALIBRATION PERIOD			VALIDATION PERIOD		
SCORE	KGE (-)	R (-)	RRMSE (%)	KGE (-)	R (-)	RRMSE (%)
CALIBRATED SECTIONS						
10	0.78	0.78	30	0.74	0.80	38
9	0.62	0.75	71	0.67	0.85	77
6	0.83	0.84	39	0.73	0.84	46
4	0.77	0.78	46	0.72	0.75	50
11	0.82	0.82	44	0.70	0.86	51
SECTIONS NOT USED FOR CALIBRATION						
1	-3.26	0.08	137	0.20	0.44	96
2	-0.57	0.48	118	0.40	0.53	89
3	0.16	0.71	83	0.39	0.70	72
5	-1.49	0.24	368	-1.26	0.31	358
7	0.53	0.68	71	0.20	0.70	81
8	0.80	0.84	36	0.77	0.84	39

830

831

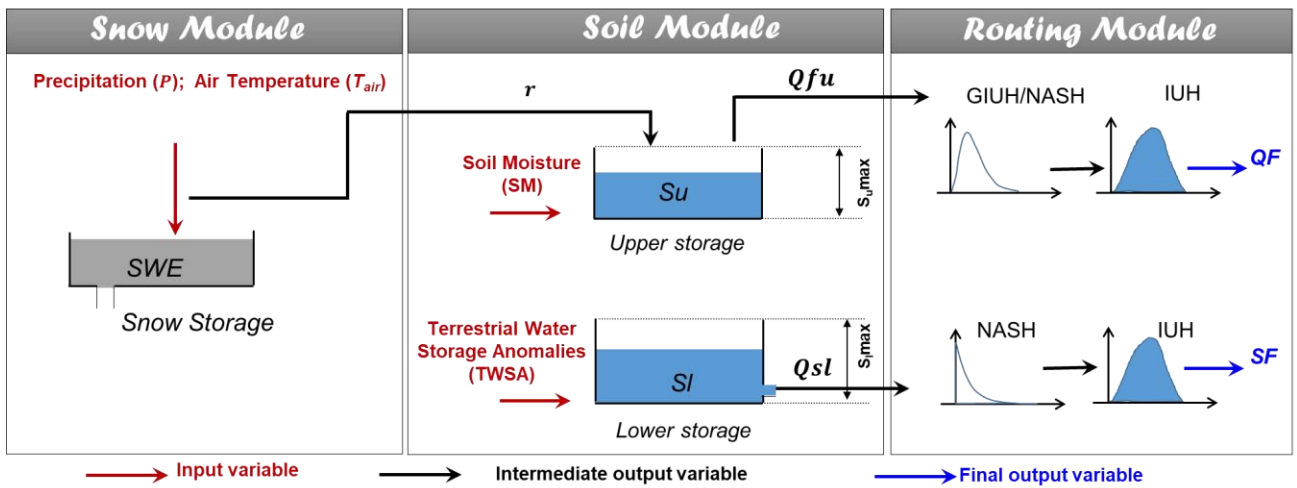
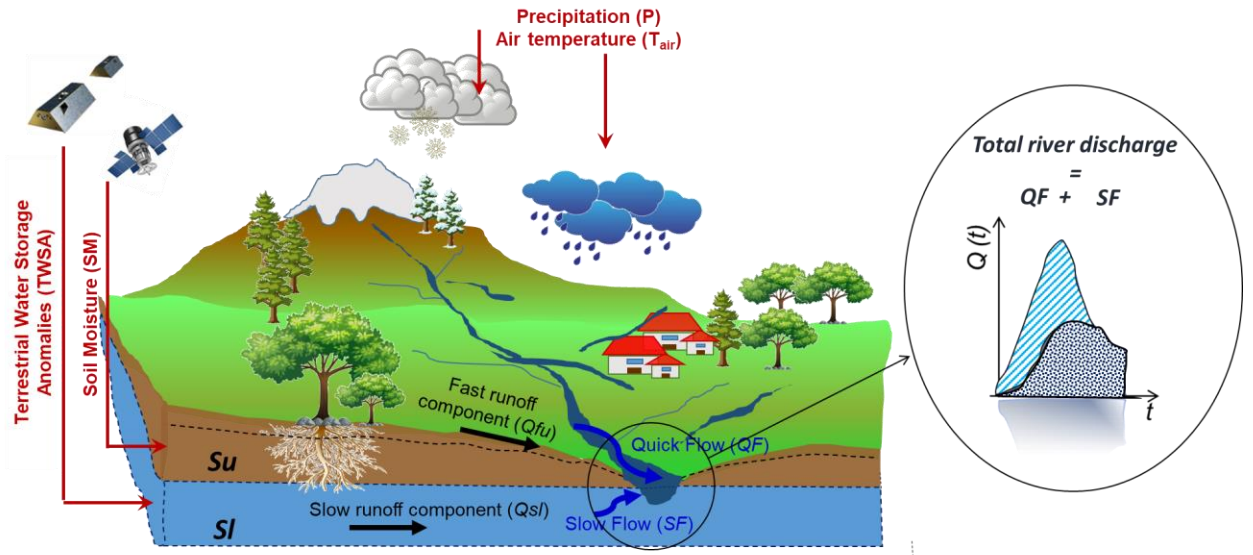
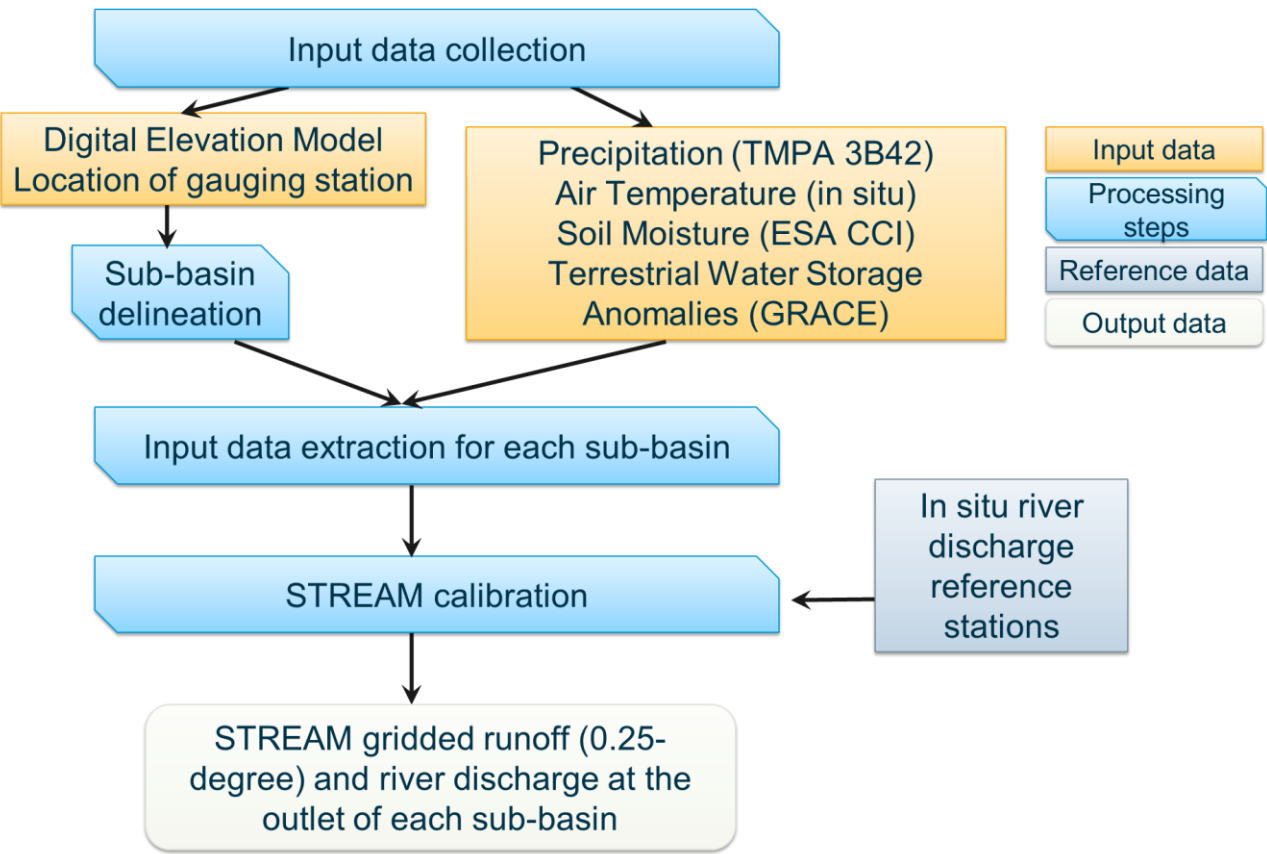


Figure 1. Configuration of the STREAM v1.3 model adopted for total runoff estimation. The model includes three modules, the snow module allowing to separate snowfall from precipitation, the soil module that simulates the slow and quick runoff components (Q_{su} and Q_{fu} , respectively) and the routing module for flood simulation. Red arrows indicate input variables; black arrows indicate intermediate output variables; blue arrows indicate final output variables. The components Q_{fu} and Q_{su} are computed by using satellite P , soil moisture and TWSA data as input to the soil module. Please refer to text for symbols.

841



842

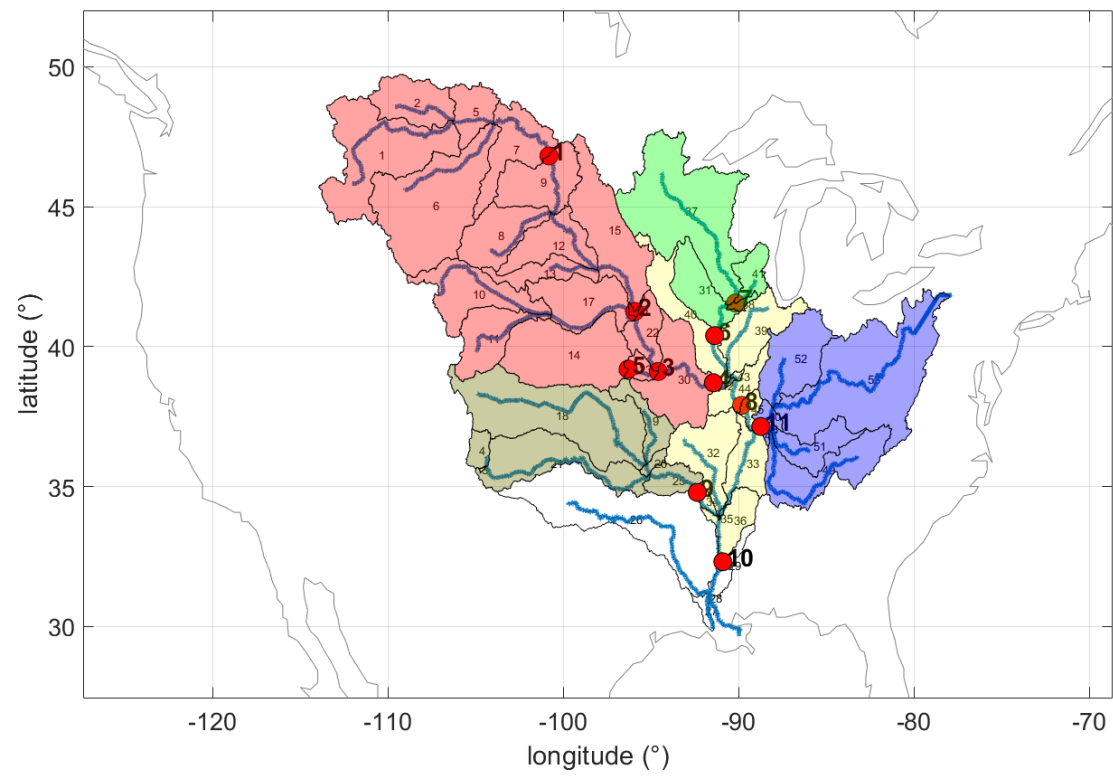
843

844

845

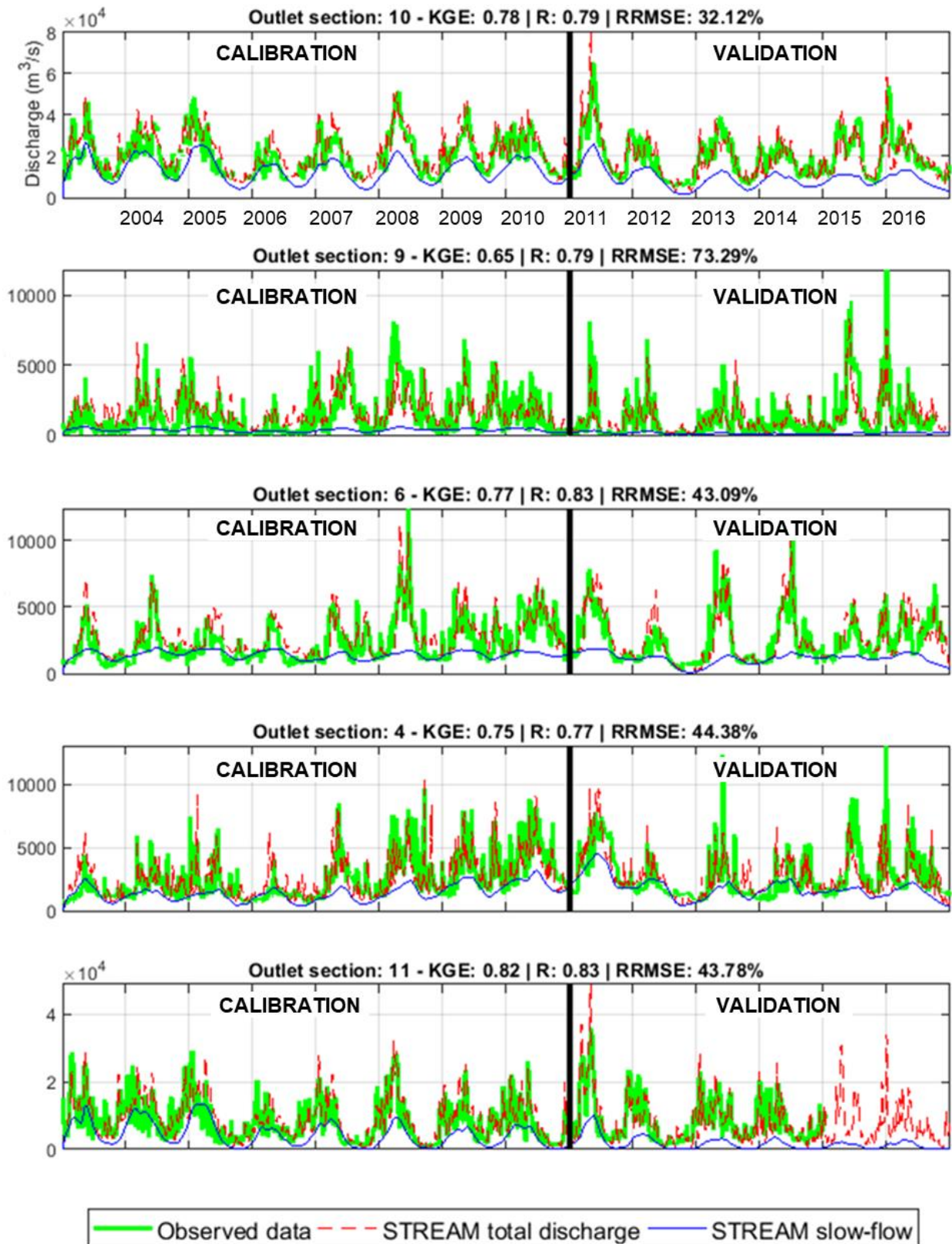
Figure 2. Processing steps of the STREAM v1.3 model.

846



847

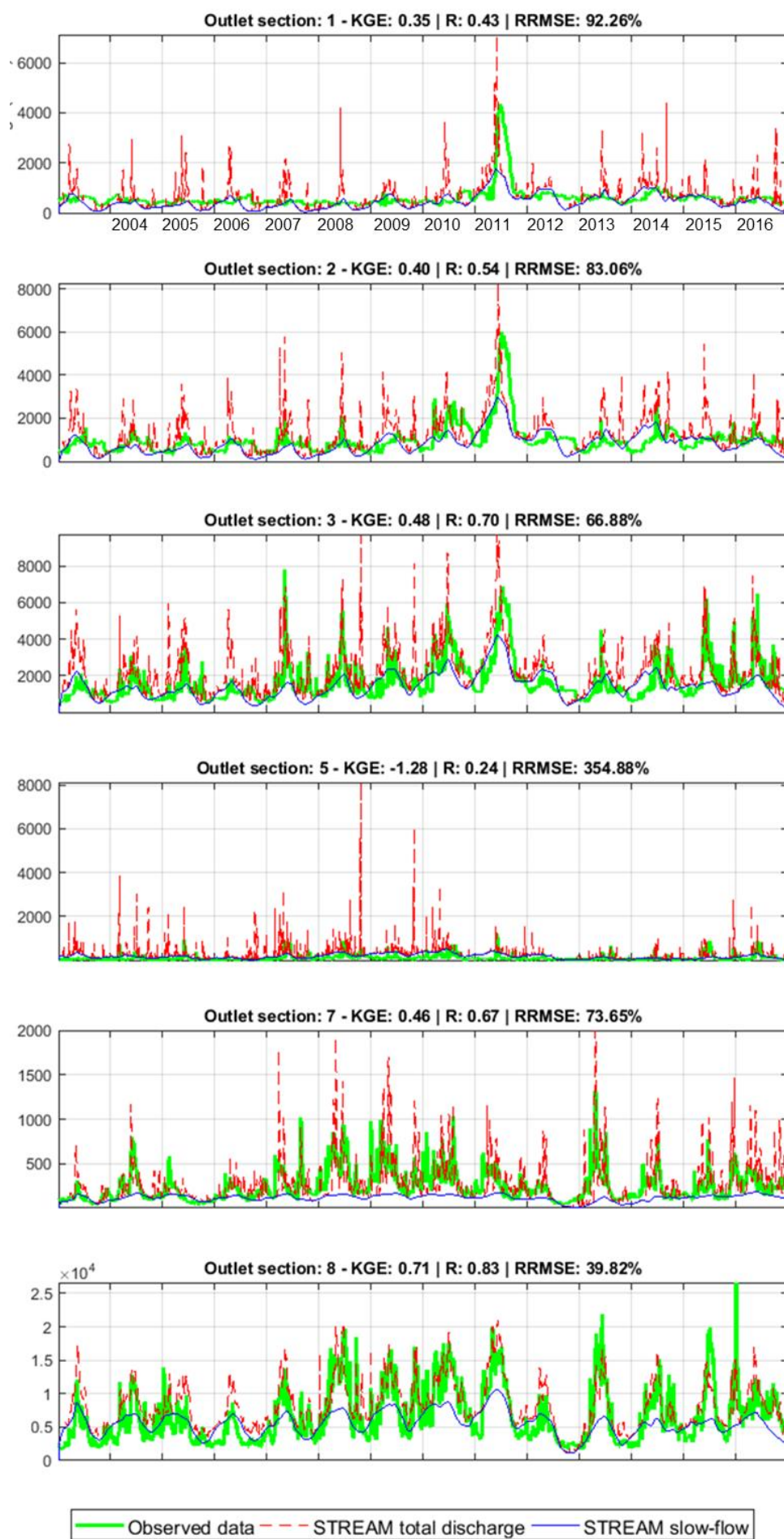
848 Figure 3. Mississippi sub-basin delineation. Red dots indicate the location of the discharge gauging
849 stations; different colours identify different inner sections (and the related contributing sub-basins)
850 used for the model calibration.
851



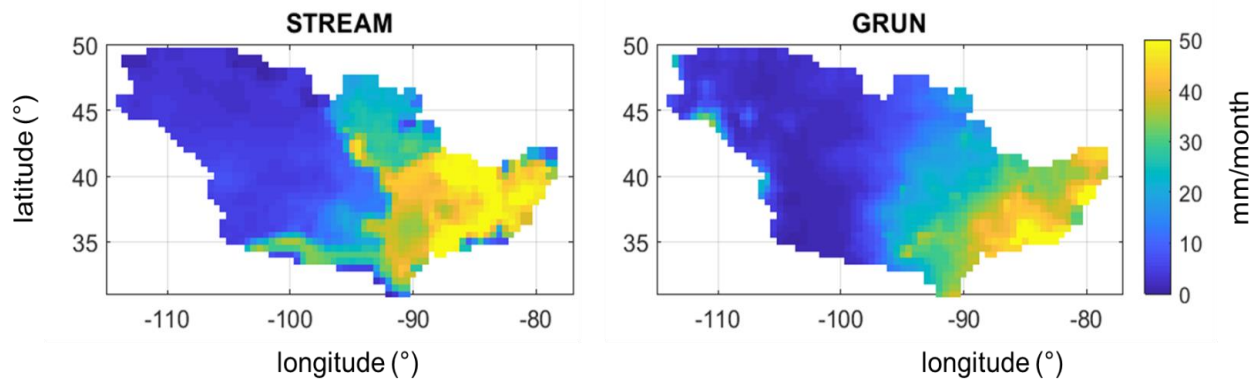
852

853 Figure 4. Comparison between observed and simulated river discharge time series over the five
 854 calibrated sections over Mississippi river basin. Performance scores at the top of each plot refer to
 855 the entire study period (2003–2016).

856



858
860 Figure 5. Comparison between observed and simulated river discharge time series over the gauged
861 sections not used in the calibration phase. Performance scores at the top of each plot refer to the entire
862 study period (2003–2016).
863



864

865 Figure 6. Mississippi river basin: mean monthly runoff for the period 2003–2014 obtained by
 866 STREAM v1.3 and GRUN models.

867

869 Table 1A. Description of STREAM v1.3 parameters, belonging module, variability range and unit.

Parameter	Description	Module	Range Variability	Unit
Cm	degree-day coefficient	Snow	0.1/24-3	[-]
α	exponent of infiltration	Soil	1-30	[-]
T	characteristic time length	Soil	0.01-80	[days]
β	coefficient relationship slow runoff component and TWSA	Soil	0.1-20	[mm h-1]
m	exponent in the relationship between slow runoff component and TWSA	Soil	1-15	[-]
γ	parameter of GIUH	Routing	0.5-5.5	[-]
C	Celerity	Routing	1-60	[km h-1]
D	Diffusivity	Routing	1-30	[km2 h-1]

870